Article

Cephalometric Analysis in Studying the Position of the Hyoid Bone and the Upper Respiratory Tract Status in Patients with Occlusion Issues.

Dmitry Domenyuk[1], Taisiya Kochkonyan[2], Stanislav Domenyuk[3]

[1] Stavropol State Medical University, Stavropol, Russia

[2] Kuban State Medical University, Krasnodar, Russia

[3] North Caucasus Federal University, Stavropol, Russia

* Correspondence: domenyukda@mail.ru

domenyukda@mail.ru, https://orcid.org/0000-0003-4022-5020 (D.D)

kochkonyantaisiya@mail.ru,https://orcid.org/0000-0003-1613-3425(T.K)

sdomenyuk@bk, https://orcid.org/0000-0001-5239-4601(S.D)

Citation: Domenyuk D., Kochkonyan T., Domenyuk S. Cephalometric Analysis in Studying the Position of the Hyoid Bone and the Upper Respiratory Tract Status in Patients with Occlusion Issues.Otorhinolaryngology, Head and Neck Pathology (ORLHNP). 2024; 3 (1): 43-60. https://doi.org/10.59315/ORLHNP.2024-3-1.43-60

Academic Editor: Valentin Popadyuk

Received: 20.01.2024
Revised: 22.02.2024
Accepted: 25.02.2024
Published: 30.03.2024

Publisher's Note: International Society for Clinical Physiology and Pathology (ISCPP) stays neutral with regard to jurisdictional claims in published maps and institutional affiliations.

Copyright: © 2024 by the authors. Submitted for possible open access publication.

Abstract:

Rationale. Occlusion sagittal issues come accompanied with morphological disorders affecting the facial skeleton, the shape and size of dental arches, the temporomandibular joint elements, disturbed chewing function, swallowing, breathing, speech production, as well as change involving the posture balance. Cephalometric analysis offers the most reliable and promising option in studying the hyoid bone position and the upper respiratory tract (URT) status.

Aim of study. This study was carried out aiming at improving the diagnostics reliability, when dealing with patients featuring occlusion pathology, through studying the hyoid bone position and the upper respiratory tract status relying on the cephalometric analysis of the head lateral telerentgenograms (TRG).

Materials and methods. The study involved 76 children aged 15-17 bearing the diagnosis of *Distal occlusion* (DO); the patients were divided into 2 subgroups – Subgroup 1 (n=41) where the patients had DO combined with sagittal incisive disocclusion and Subgroup 2 (n=35) who featured DO along with deep incisive disocclusion. Adolescents (n=34) revealing physiological occlusion were the comparison group. The cephalometric analysis of the head profile TRGs (OnDemand3D™ Dental software; CEPH module) employed linear, angular and index parameters in order to identify individual features of the craniofacial structure as well as the os hyoideum position. The degree of the URT narrowing at the nose and oropharynx level was determined via 3D reconstruction of cone beam computed tomograms (CBCT) based on a visual colorimetric scale.

Results and discussion. The cephalometric analysis of the linear, angular and index indices of the head lateral TRGs obtained through examining adolescents with distal occlusion revealed mutual effects of gnathic, cranial and dental alveolar factors. The hyoid bone upward displacement in adolescents with DO, if compared to children with physiological occlusion, was obvious through a statistically significant ($p \leq 0.05$) decrease in the Me values of H-S (by 13.69%-14.55%); H-RGn (by 21.91%-22.57%); H-MR (by 47.57% and 54.76%); ‹H-Me-MP (by 32.38%-34.98%). As far as the os hyoideum backward shift is concerned, it was to be seen from a significant ($p \leq 0.05$) decrease in the Me values of H-CIII (by 25.42%-26.05%) with an increase in ‹HGo-NM (by 9.94%-10.34%). The changes identified in the hyoid bone topography in children with DO came combined with a dynamic narrowing of the URT, that manifesting itself through a significant ($p \leq 0.05$) reduction in the total volume of the respiratory tract and the cross-sectional area.

Conclusion.The URT volume measurement carried out with CBCT, the hyoid bone topography evaluation, identifying the tongue position and size along with doing the same for the cervical vertebrae and for the posture compensation degree, allow the dentist to take an objectively reliable approach to diagnosing and treating dental pathologies, which, in turn, will improve the overall quality of dental treatment. The retroposition of the lower jaw results in a compressed upper respiratory tract, which will facilitate the development of compensatory changes in the cranio-vertebral joint, that expressing in the anterior position of the head. Identifying due normative parameters and the status of the URT, as well as the connection with the dental structure status, for cases falling within norm or disturbed occlusion range, will require further research.

Keywords: cone beam computed tomography, upper respiratory tract, cephalometric analysis, hyoid bone position, distal occlusion, lateral telerentgenogram, craniofacial area.

1. Introduction

The current progress in fundamental science and the widespread introduction of innovation-based technologies into Medicine nowadays offer many more options for employing in vivo imaging methods, both in anatomical and topographic & anatomic studies [1-5].

Advanced study of morphological and topographic features, dimensional values, individual anatomic variability of the hyoid bone structure, as well as links with the craniofacial region structures and ENT organs is of great research and applied importance for otorhinolaryngology, maxillofacial surgery, surgical dentistry, orthognathic surgery, orthodontics, and forensic medicine [5-8].

The hyoid bone, as an element connecting the neck deep muscles and the oral cavity bottom, plays an important role in swallowing, speech production, complex head turns, whereas clinicians' lacking knowledge of the hyoid bone typical anatomy and topography, in view of the constitution type, may serve a serious obstacle when diagnosing closed neck injuries, increase the risk of damage to vital organs, as well as make it difficult to perform successful intubation, as well as lead to internal injuries of the larynx and trachea during medical procedures and manipulations [9,10].

The focus of otorhinolaryngologists' and dentists' attention is the respiratory tract status, viewed as one of the key factors behind the growth and development of maxillofacial structures [11].

Given the functional integrity of the craniofacial area anatomical structures, experts do not identify the primary etiopathogenetic mechanism, which results in obstructed upper respiratory tract or dental anomalies. On the one hand, the functional imbalance arising from the nasopharyngeal tonsils hypertrophy, curved nasal septum, foci of chronic infection affecting the ENT organs, allergic rhinitis, nasal polyps, and congenital abnormalities involving internal organs contribute to the development of oral breathing, disturbed tightness of the oral cavity with lacking negative pressure in it; non-physiological (lower) position of the tongue; muscle discoordination resulting in the posterior position of the lower jaw; the vertical type of the facial skeleton growth; narrowing upper dental arch in the distal – and elongated in the frontal – sections. On the other hand, dental anomalies caused by maxillofacial malformations due to growth issues in the embryonic period, functional disorders of chewing and facial muscles, adverse external factors and poor habits through the period of developing the temporary and permanent bite, change the physiological ratio of the head, jaw bones and tongue, initiating narrowing (stenosis) of the airways [12-20].

Identifying the upper respiratory tract (URT) status employing the skull TRG in the lateral projection allows obtaining details regarding the width of the lumen along the sagittal. The authors of the study have proposed various methods for assessing the URT patency, which differ in the number (topography) of the reference points (lines) and the measurement levels of cross-sections [21,22]. Despite the controversial issues in detecting the URT boundaries due to the variability and mobility of soft tissues and bone structures around the respiratory tract, as well as to the normative values of the URT lumen in various areas, respiratory failures can be diagnosed in case of a 40+% reduction in the URT cross-sectional area [23].

High-tech radiation methods, such as computed tomography (CT) and magnetic resonance imaging (MRI) allows performing 3D diagnostics of URT while maintaining the volume of the object and the possibility of post-contrast thin-slice imaging in any of the planes at high resolution, taking into account contour irregularities [24-27]. 3D reconstruction with cone beam computed tomography (CBCT), which features a lower radiation load, is the most reliable and diagnostically valuable method of measuring URT; besides, unlike MRI, CBCT offers an advantage in assessing the status of bone structures and foreign bodies [28-30]. The reference points that are described in the scientific literature, which allow identifying linear and angular parameters for assessing the hyoid bone topography in patients with dental anomalies, are not numerous and of a disparate nature, which was the reason explaining the rationale of this study.

Aim of study: to study the topography of the hyoid bone in adolescents with distal occlusion, while relying on cephalometric analysis of head telerentgenograms (TRG) in the lateral projection.

2. Patients and Methods

The premises of the Orthodontic Department (Pediatric Dental Polyclinic, Stavropol State Medical University / StSMU) and of the Department for General Practice Dentistry and Pediatric Dentistry of StSMU were used (2018-2023) to carry out a clinical X-ray examination and comprehensive treatment involving 76 patients (29 males, 47 females) with gnathic distal occlusion of the dentition caused by inferior micrognathia and posterior position of the lower jaw (main group). The inclusion criteria for the main group were: age – 15-17; distal occlusion (K07.20 by ICD-10); mandible micrognathia (K07.04 by ICD-10); mandible retrognathia (K07.13 by ICD-10); skeletal II class by E. Angle (∠SNB value less than 78°, ∠ANB value more than 4°); ratios for the first molars - more than 1 mm; incisor retraction; incisor protrusion; informed voluntary consent obtained from the patients' parents (legal representatives) for orthodontic treatment; no congenital maxillofacial malformations; no bone diseases; no mental disorders.

The diagnosis was set relying on the outcomes of clinical and additional re-search methods. Based on the classification of abnormal dentition occlusion(by Prof. L.S. Persina, Member of the Russian Academy of Medical Sciences, 1989), subject to a recommendation by the resolution of the X Congress of the Russian Professional Society of Orthodontists (2006), the patients of the main

group were divided into two subgroups: Subgroup 1 – children with distal occlusion accompanied by sagittal incisive disocclusion (n=41; 13 - males, 28 – females); Subgroup 2 – children with distal occlusion accompanied by deep incisive disocclusion (n=35; 14 - males, 21 – females). The comparison group (n=34; 12 - males, 22 – females) included patients with physiological types of occlusive relationships (of similar age) (Class I by E. Angle, ∠SNB - 80±2°, ∠ANB - 2±2°).

Since there was no statistically significant difference resulting from the gender, cephalometric studies data obtained in females and males were combined. X-Ray examinations (OPTG, TRG of the head in the lateral projection, CBCT) were performed employing a KaVo Orthopantomograph™ OP 3D digital X-ray diagnostic system with the 3D-tomography function with the conventional occlusion at standard head positioning in the cephalostat (radiation load – 1.8-3.1 microsievert). Further cephalometric analysis of the head TRG in the lateral projection (OnDemand3D Dental software, CEPH module) employed 39 values pertaining to the dental parameters, the skeletal status, as well as soft-tissue and skeletal profiles. Of the total number of parameters that serve to identify the individual dental morphological features, 11 linear, 10 angular and 2 index values were selected as the most significant in terms of diagnosing distal occlusion. To identify the alteration degree in the hyoid bone topography, 7 linear and 2 angular indicators describing the position of os hyoideum relative to the cervical spine and bones of the facial skull, were specifically identified (Table 1, Fig. 1-3).

Parameters	Title
Skeletal parameters	
Linear parameters (mm)	
N-Me	Anterior total morphological height of the face
N-ANS	Front upper face height
N-Se	Length of the anterior aspect of the skull base
N-Gn	Anterior height of the facial skull
A*-SnP	Upper jaw length
ANS-Me	Front lower face height
S-Go	Posterior face height
Pg-Go	Length of the base of the mandible
Co-Go	Length of the mandibular branch
H-S	Distance from the body of the hyoid bone to the equidistant point of the contour of the Turkish saddle
H-C_{III}	Distance from the body of the hyoid bone to the lowest point of the anterior edge of the body of the third cervical vertebrae
H-RGn	Distance from the body of the hyoid bone to the posterior point of the chin symphysis
H-MP	Length of the perpendicular from the body of the hyoid bone to the plane of the base of the mandibular body
H-N	Distance from the body of the hyoid bone to the anterior point of the nasolabial suture in the sagittal plane
H-A	Distance from the body of the hyoid bone to the distally located point on the anterior contour of the apical base of the maxilla
H-B	Distance from the body of the hyoid bone to the distally located point on the anterior contour of the apical base of the mandible
Index parameters (%)	
N-ANS/ANS-Me	Ratio of anterior upper to anterior lower face height
S-Go/N-Me	Ratio of posterior facial height to total anterior facial height
Angular parameters (°)	
‹SNB	Position of the apical base of the mandible relative to the anterior part of the skull base sagittally
‹SNA	Position of the apical base of the maxilla relative to the anterior part of the skull base sagittally
‹ANB	Ratio of the apical bases of the jaws relative to the skull base
‹Go	Angle of the mandible
‹SN-Pog	Anteroposterior position of the chin relative to the anterior skull base
‹Beta	Ratio of upper and lower jaws, skeletal class

‹NSe-MP	Position of the mandibular body base plane in relation to the length of the anterior skull base
‹NSe-SpP	Position of the plane of the base of the maxilla in relation to the length of the anterior skull base
Σ Bjork	Sum of angles by Bjork = ‹NSeAr + ‹SeArGo + ‹ArGoMe
‹H-Me-MP	Inclination of the body of the hyoid bone to the plane of the base of the mandibular body
‹HGo-HMe	Position of the body of the hyoid bone in relation to the plane of the base of the mandibular body
Dental parameters	
Linear parameters (mm)	
Overbite	Depth of cutter overlap
Overjet	Sagittal cleft size
Angular parameters (°)	
‹U1-L1	Interincisal Angle

Table 1. Linear, index and angular parameters studied at head TRG in lateral projection through cephalometric analysis

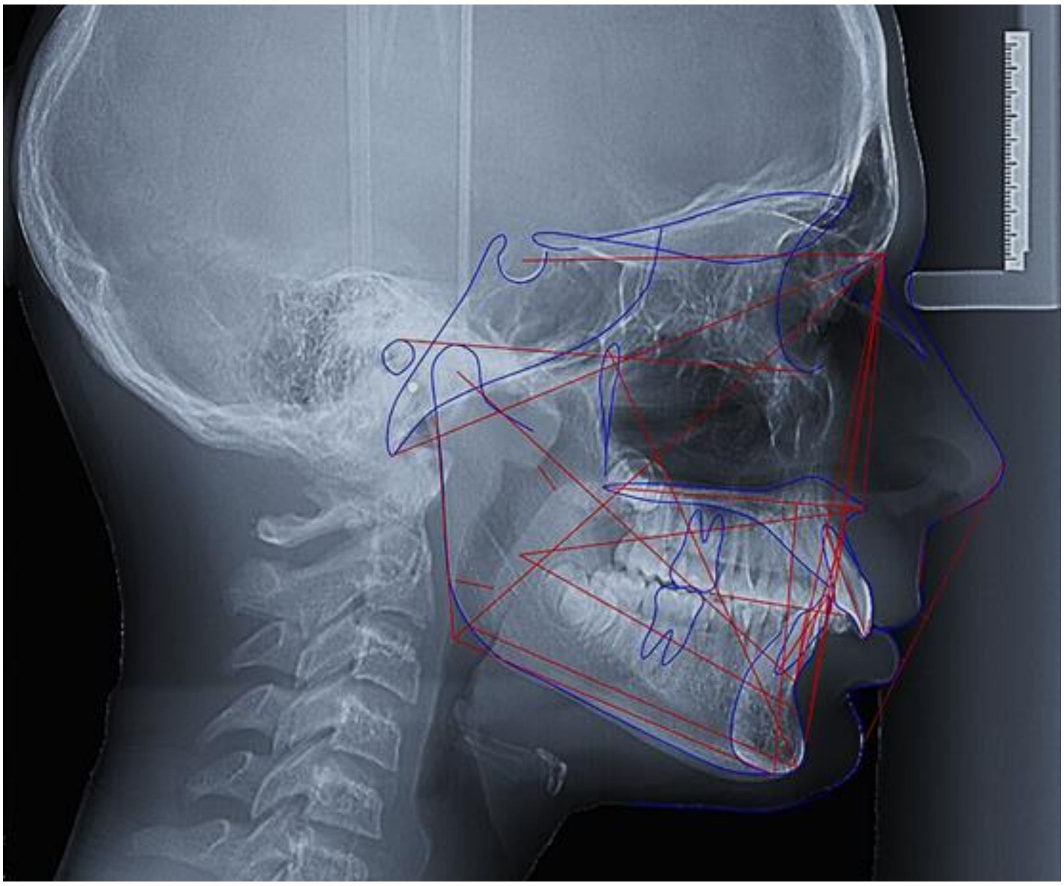

Fig. 1. Head TRG examination scheme; lateral projection; patient M., 16 y.o.; distal occlusion accompanied by deep incisive disocclusion.

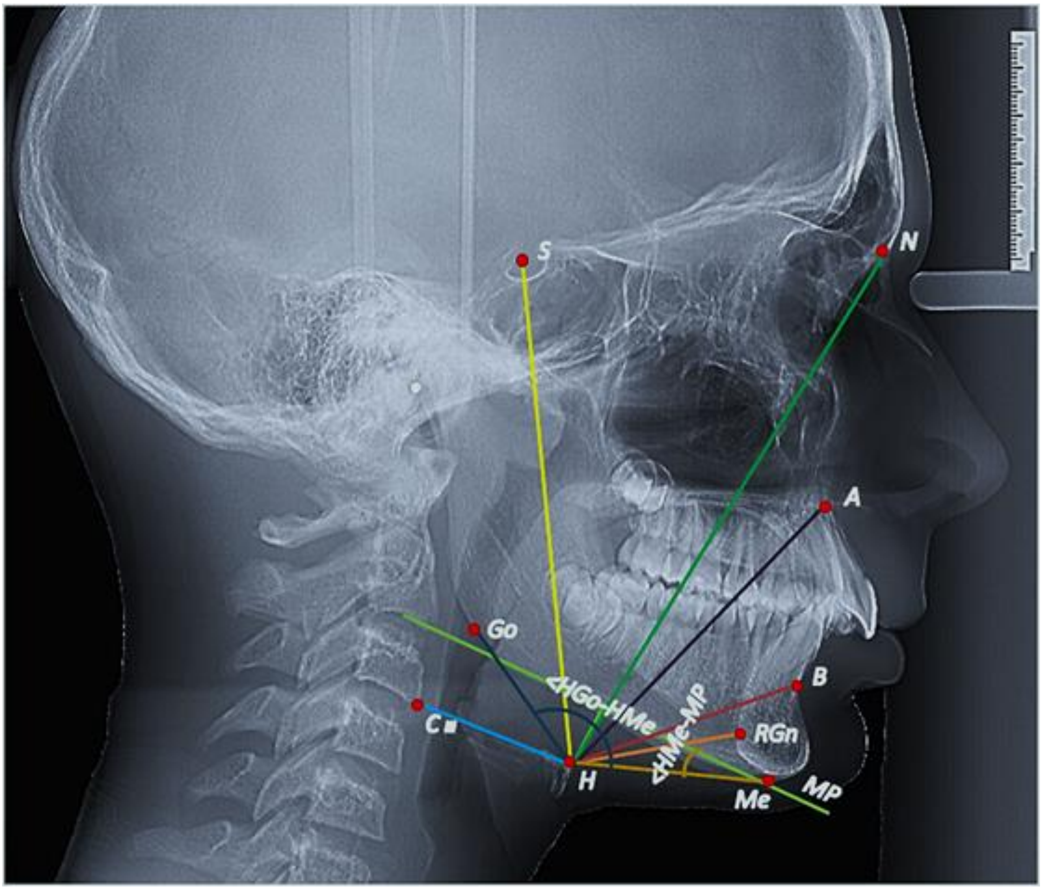

Fig. 2. Location of reference points, linear and angular parameters for determining the topography of the hyoid bone on a head TRG; lateral projection; patient M., 16 y.o.; distal occlusion accompanied by deep incisive disocclusion.

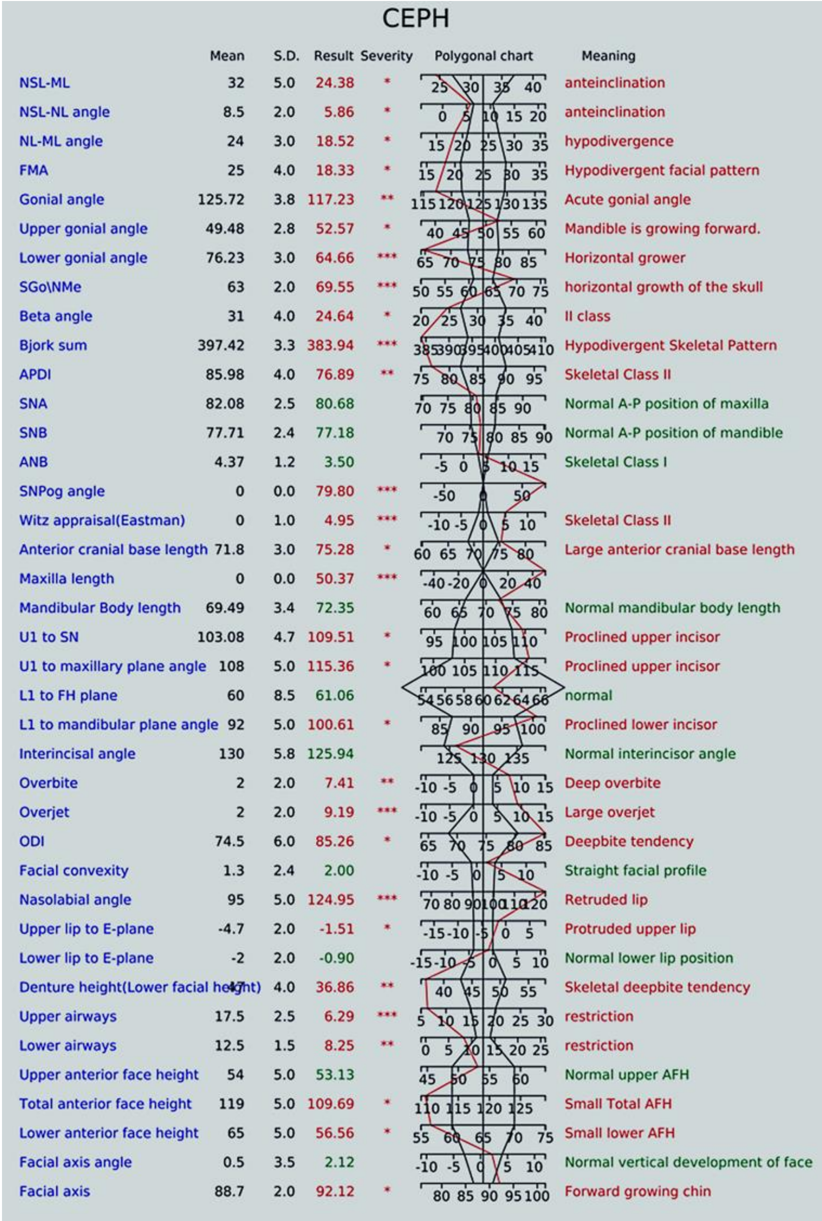

CEPH

	Mean	S.D.	Result	Severity	Polygonal chart	Meaning
NSL-ML	32	5.0	24.38	*		anteinclination
NSL-NL angle	8.5	2.0	5.86	*		anteinclination
NL-ML angle	24	3.0	18.52	*		hypodivergence
FMA	25	4.0	18.33	*		Hypodivergent facial pattern
Gonial angle	125.72	3.8	117.23	**		Acute gonial angle
Upper gonial angle	49.48	2.8	52.57	*		Mandible is growing forward.
Lower gonial angle	76.23	3.0	64.66	***		Horizontal grower
SGo\NMe	63	2.0	69.55	***		horizontal growth of the skull
Beta angle	31	4.0	24.64	*		II class
Bjork sum	397.42	3.3	383.94	***		Hypodivergent Skeletal Pattern
APDI	85.98	4.0	76.89	**		Skeletal Class II
SNA	82.08	2.5	80.68			Normal A-P position of maxilla
SNB	77.71	2.4	77.18			Normal A-P position of mandible
ANB	4.37	1.2	3.50			Skeletal Class I
SNPog angle	0	0.0	79.80	***		
Witz appraisal(Eastman)	0	1.0	4.95	***		Skeletal Class II
Anterior cranial base length	71.8	3.0	75.28	*		Large anterior cranial base length
Maxilla length	0	0.0	50.37	***		
Mandibular Body length	69.49	3.4	72.35			Normal mandibular body length
U1 to SN	103.08	4.7	109.51	*		Proclined upper incisor
U1 to maxillary plane angle	108	5.0	115.36	*		Proclined upper incisor
L1 to FH plane	60	8.5	61.06			normal
L1 to mandibular plane angle	92	5.0	100.61	*		Proclined lower incisor
Interincisal angle	130	5.8	125.94			Normal interincisor angle
Overbite	2	2.0	7.41	**		Deep overbite
Overjet	2	2.0	9.19	***		Large overjet
ODI	74.5	6.0	85.26	*		Deepbite tendency
Facial convexity	1.3	2.4	2.00			Straight facial profile
Nasolabial angle	95	5.0	124.95	***		Retruded lip
Upper lip to E-plane	-4.7	2.0	-1.51	*		Protruded upper lip
Lower lip to E-plane	-2	2.0	-0.90			Normal lower lip position
Denture height(Lower facial height)	47	4.0	36.86	**		Skeletal deepbite tendency
Upper airways	17.5	2.5	6.29	***		restriction
Lower airways	12.5	1.5	8.25	**		restriction
Upper anterior face height	54	5.0	53.13			Normal upper AFH
Total anterior face height	119	5.0	109.69	*		Small Total AFH
Lower anterior face height	65	5.0	56.56	*		Small lower AFH
Facial axis angle	0.5	3.5	2.12			Normal vertical development of face
Facial axis	88.7	2.0	92.12	*		Forward growing chin

Fig. 3. Final computer analysis pattern of head TRG; lateral projection; patient M., 16 y.o.; with distal occlusion accompanied by deep incisive disocclusion (OnDemand3D™ Dental program, CEPH module).

The statistical analysis was performed using the Version 21.0 Microsoft Office Excel software package and Statistics 22.0 IBM ® SPSS ® (StatSoft Inc, USA). The hypothesis normality of the quantitative features distribution was checked through the Kolmogorov-Smirnov criterion employing the Lilliefors test as well as Shapiro-Wilk's test. The studied indicators predominantly had significant deviations from normality, so nonparametric criteria were used to identify the median (Me), minimum (Min) and maximum (Max) values, as well as the 10th, 25th (Q1), 75th (Q3), 90th percentiles. The comparisons of independent samples were set with the Mann–Whitney U test (the critical significance p level was taken as 0.05). Further pairwise comparison of the groups was performed using the Mann–Whitney U test with Bonferroni correction.

3. Results

Tables 2-4 contain the results of the head TRG cephalometric analysis in the lateral projection.

Table 2. Linear, index and angular parameters studied at head TRG in lateral projection; patients with physiological occlusion (comparison group)

Parameters	Me	Min	Max	Percentiles			
				Q-25	Q-75	Q-10	Q-90
Skeletal parameters							
Linear parameters (mm)							
N-Me	114,04	109,51	118,72	113,17	115,49	112,09	116,58
N-ANS	52,97	48,62	57,49	51,54	54,06	50,16	54,91
N-Se	69,75	64,43	75,22	68,03	71,64	66,71	73,83
N-Gn	124,52	116,77	130,04	122,09	126,14	118,82	127,95
A*-SnP	45,08	43,63	47,21	44,73	45,90	44,05	46,74
ANS-Me	64,82	60,19	69,13	63,18	65,91	61,56	66,84
S-Go	73,01	69,28	78,31	72,28	75,18	71,24	76,43
Pg-Go	72,46	67,93	79,07	71,84	74,65	69,04	76,99
Co-Go	53,18	49,27	57,01	51,77	54,43	50,36	56,14
Index parameters (%)							
N-ANS/ANS-Me	81,72	80,78	83,16	81,57	82,02	81,48	82,15
S-Go/N-Me	64,02	63,26	65,96	63,87	65,09	63,56	65,56
Angular parameters (°)							
‹SNB	79,67	75,94	84,13	78,52	81,05	77,26	82,81
‹SNA	82,14	78,06	89,19	80,89	84,02	79,93	85,44
‹ANB	2,26	-1,07	6,41	1,57	3,40	0,13	4,91
‹Go	129,58	122,94	137,65	126,83	132,16	125,02	134,59
‹SN-Pog	80,38	68,70	88,23	78,92	83,07	76,64	85,33
‹Beta	28,81	21,32	39,78	27,97	33,18	26,71	35,25
‹NSe-MP	31,07	27,15	38,36	29,94	33,53	28,89	35,70
‹NSe-SpP	8,28	4,63	12,06	7,06	10,15	5,94	10,82
Σ Bjork	393,41	379,54	401,12	390,73	395,24	383,76	399,62
Dental parameters							
Linear parameters (mm)							
Overbite	2,13	0,76	3,84	1,42	2,81	1,09	3,38
Overjet	2,46	0,54	5,12	1,56	3,31	1,23	4,04
Angular parameters (°)							
‹U1-L1	135,62	131,28	139,09	133,84	136,96	132,70	137,86

Table 3. Linear, index and angular parameters studied at head TRG in lateral projection; patients with distal occlusion accompanied by sagittal incisive disocclusion (Sub-group 1, main group)

Parameters	Me	Min	Max	Percentiles			
				Q-25	Q-75	Q-10	Q-90
Skeletal parameters							
Linear parameters (mm)							
N-Me	111,42	107,03	115,12	110,13	112,51	108,94	113,37
N-ANS	48,19**	43,97**	54,31**	47,34**	49,26**	46,01**	51,41**
N-Se	70,88	63,26	76,19	68,71	73,03	65,83	74,52
N-Gn	112,45	100,91	123,58	109,63	116,90	107,16	120,72

A*-SnP	50,37*	44,19*	57,04*	48,84*	52,05*	47,13*	54,28*
ANS-Me	65,38	60,76	71,12	64,48	66,61	63,24	68,74
S-Go	69,17	64,91	76,05	67,89	70,73	66,29	72,69
Pg-Go	73,76	65,52	80,93	72,01	75,92	68,39	78,24
Co-Go	57,24	49,83	64,65	55,69	59,19	53,18	62,07
Index parameters (%)							
N-ANS/ANS-Me	73,71	72,47	76,36	73,42	73,95	72,75	74,79
S-Go/N-Me	62,08	60,65	66,06	61,64	62,86	60,85	64,12
Angular parameters (°)							
‹SNB	73,05**	69,59**	77,18**	72,14**	74,49**	71,08**	75,91**
‹SNA	82,39	77,81	90,58	81,07	84,51	79,14	87,08
‹ANB	5,95	4,17	8,22	5,16	6,54	4,42	7,13
‹Go	120,27	113,96	126,42	118,89	121,93	117,16	124,51
‹SN-Pog	76,57	67,11	84,83	74,20	79,05	72,39	82,44
‹Beta	19,86*	16,32*	23,07*	18,73*	20,77*	17,64*	21,49*
‹NSe-MP	28,38	25,09	32,41	27,23	30,12	26,01	31,35
‹NSe-SpP	8,62	5,27	11,88	7,52	9,79	6,41	10,63
Σ Bjork	387,74	378,96	398,35	385,09	392,87	382,53	396,28
Dental parameters							
Linear parameters (mm)							
Overbite	3,05	0,94	4,17	2,62	3,27	1,57	3,66
Overjet	6,61*	4,49*	8,74*	6,19*	6,98*	5,53*	7,91*
Angular parameters (°)							
‹U1-L1	116,88**	114,17**	119,73**	115,96**	117,52**	115,04**	118,81**

Note: * – reliability of statistical differences at the level of p≤0.05 by the Mann-Whitney criterion in relation to the comparison group; ** - reliability of statistical differences at the level of p≤0.01 by the Mann-Whitney criterion in relation to the comparison group.

Table 4. Linear, index and angular parameters studied at head TRG in lateral projection; patients with distal occlusion accompanied by deep incisive disocclusion (Subgroup 2, main group)

Parameters	Me	Min	Max	Percentiles			
				Q-25	Q-75	Q-10	Q-90
Skeletal parameters							
Linear parameters (mm)							
N-Me	111,81	107,69	116,74	110,54	113,03	109,12	114,13
N-ANS	49,37**	44,96**	56,05**	48,61**	50,58**	47,19**	52,64**
N-Se	71,24	64,51	75,93	69,58	73,41	66,02	74,86
N-Gn	113,09	102,54	124,17	110,76	118,12	108,08	121,26
A*-SnP	49,63*	43,98*	56,51*	48,72*	51,83*	46,85*	54,77*

ANS-Me	63,72	59,18	69,97	62,87	65,01	61,59	67,09
S-Go	72,66	68,14	79,21	71,52	74,48	69,94	76,39
Pg-Go	74,35	66,27	81,28	72,63	76,17	69,04	78,87
Co-Go	56,71	48,94	63,37	54,90	60,08	52,54	61,73
Index parameters (%)							
N-ANS/ANS-Me	77,48	75,97	80,11	77,36	77,80	76,62	78,46
S-Go/N-Me	64,98	63,27	67,85	64,70	65,89	64,09	66,93
Angular parameters (°)							
‹SNB	76,12**	71,93**	78,97**	75,36**	76,81**	73,84**	77,69**
‹SNA	81,14	77,02	88,45	80,11	82,96	78,69	85,93
‹ANB	4,89	2,94	7,31	4,14	5,58	3,77	6,02
‹Go	121,46	115,03	127,71	119,22	123,80	117,94	125,46
‹SN-Pog	77,31	68,26	85,17	75,16	79,72	73,08	83,05
‹Beta	20,65*	16,16*	23,52*	19,49*	21,91*	18,08*	22,32*
‹NSe-MP	28,17	24,88	31,79	27,52	29,84	26,35	30,93
‹NSe-SpP	8,48	5,46	11,61	7,87	10,02	6,74	10,82
Σ Bjork	389,04	380,13	399,59	386,18	393,40	383,72	397,01
Dental parameters							
Linear parameters (mm)							
Overbite	6,75*	4,81*	7,83*	6,13*	7,22*	5,38*	7,60*
Overjet	4,64	2,92	5,78	4,33	5,05	3,77	5,34
Angular parameters (°)							
‹U1-L1	133,15	130,44	137,82	132,06	134,34	131,69	136,53

Note: * – reliability of statistical differences at the level of $p \leq 0.05$ by the Mann-Whitney criterion in relation to the comparison group; ** - reliability of statistical differences at the level of $p \leq 0.01$ by the Mann-Whitney criterion in relation to the comparison group.

The results of the dental apparatus evaluation in patients with distal occlusion accompanied by sagittal and deep incisive disocclusion (if compared against similar parameters in patients with physiological occlusion), as is seen from the head TRG in the lateral projection, revealed the following features:

– The N-Me, N-Se, Pg-Go linear gnathic and cranial parameters in the groups match the respective age-related reference values. If compared with the comparison group, the mandible branch (Co-Go) by Me in children of the main groups (Subgroups 1 and 2) is longer by 7.63% and 6.64% (unreliable, $p \geq 0.05$), the upper jaw (A*-SnP) is longer by 11.73% and 10.09%, respectively (reliably identified, $p \leq 0.05$), while the anterior height of the facial skull (N-Gn) was found to be reduced by 9.69% and 9.18%, respectively (unreliable, $p \geq 0.05$);

– The facial skull vertical linear parameters in the main group (Subgroups 1 and 2), if compared with the comparison group, by Me, were reduced – the anterior upper face height (N-ANS) – by 9.02% and 6.80% (reliably identified, $p \leq 0.05$), the posterior face height (S-Go) – by

5.26% and 0.48%, respectively (unreliable, p≥0.05), whereas the intergroup statistically significant differences (p≤0.05) based on the anterior lower face height (ANS-Me) have not been identified;

– The match between the ratio of the anterior upper, the anterior lower face height (N-ANS/ANS-Me), the posterior face height as well as the total anterior face height (S-Go/N-Me) and the limits of the averaged normative values with no statistically significant differences (p≤0.05) in the groups, points at a relative balance of the facial proportions;

– The value of ‹SNA found to be within the normative range is indicative of the orthognathic face type. A decrease in the ‹SNB by Me, if put against the comparison group, by 8.31% and by 4.46% (Subgroups 1 and 2, respectively) (reliably identified, p≤0.01) means a retrogenic type of face caused by the mandible retroposition, while the distal position of the mandible against the skull base also confirms an increase in ‹ANB by 163,27% and 116.37%, respectively (unreliable, p≥0.05);

– The mandibular angle (Go) values in the main group (Subgroup 1 and 2), in relation to similar values in the comparison group, taken by Me, were lower by 7.18% and 6.27% (unreliable, p≥0.05); the ‹SN-Pog values exceeding (unreliable, p≥0.05) the ‹SNB values, by Me, in Subgroup 1 and 2 of the main group, point at the anterior position of the chin protrusion. A decrease (against the comparison group) in the ‹Beta value by Me in Subgroup 1 by 31.06%, and in Subgroup 2 – by 28.32% (reliably identified, p≤0.05) means a horizontal type of jaw growth with rotation (spatial orientation) according to the anterior type;

– The parameters of the angle determining the position of the upper jaw base plane relative to the skull anterior base length (‹NSe-SpP) in the studied groups correspond to the age reference intervals. The median sum of the Bjork angles and the angle setting the position of the mandible body base plane relative to the length of the anterior skull base (‹NSe-MP), in the main group (Subgroup 1 and 2), in relation to the comparison group, were reduced by 1.44% and 1.11% (unreliable, p≥0.05), as well as by 8.66% and 9.33%, respectively (unreliable, p≥0.05).;

– The protrusion of incisors in the main group (Subgroup 1) can be seen from a statistically significant (p≤0.05) decrease in the incisor angle Me values ‹U1-L1 by 13.82% with an increase in the overjet parameters by 168.70%, and an increase in the incisor overlap depth in Subgroup 2, which makes a significant (p≤0.05) Me increase of overbite parameters by 216.90% if compared with similar values in the comparison group, while there were no significant differences detected in the angle values ‹U1-L1 in Subgroup 2.

Table 5 shows the data obtained through the cephalometric analysis of the head TRG in the lateral projection performed to identify the hyoid bone topography.

Table 5. Linear and angular parameters identifying the hyoid bone topography; cephalometric analysis, head TRG, lateral projection

Parameters, units change	Me	Min	Max	Percentiles			
				Q-25	Q-75	Q-10	Q-90
Patients in the comparison group							
H-S (mm)	101,64	94,17	107,52	98,85	104,49	96,63	105,71
H-C_{III} (mm)	36,08	31,99	39,65	34,37	37,71	33,82	38,96
H-RGn (mm)	41,16	37,54	44,82	39,78	42,55	38,49	43,78
H-MP (mm)	15,03	10,86	18,17	13,35	16,48	12,21	17,13
H-N (mm)	119,88	102,97	131,18	113,02	124,01	108,45	127,26
H-A (mm)	75,94	67,91	84,82	72,03	78,76	70,15	81,49
H-B (mm)	49,26	38,89	58,06	45,12	54,33	42,75	56,09

‹H-Me-MP (°)	18,87	14,33	23,79	17,04	20,92	15,39	22,30
‹HGo-HMe (°)	129,31	119,58	137,66	125,92	133,54	121,71	135,08
Patients of the main group of the 1st subgroup							
H-S (mm)	86,85*	80,63*	94,19*	84,38*	89,16*	83,01*	91,43*
H-C_{III} (mm)	26,91*	23,97*	29,73*	25,56*	28,04*	25,06*	28,82*
H-RGn (mm)	32,14*	28,98*	35,02*	31,25*	33,01*	30,37*	33,69*
H-MP (mm)	7,88*	5,16*	11,04*	7,09*	8,57*	6,41*	9,49*
H-N (mm)	127,98	110,07	137,13	122,02	131,35	116,84	134,90
H-A (mm)	81,17	68,14	89,08	76,36	84,21	73,01	86,63
H-B (mm)	46,03	29,35	54,09	41,48	49,27	36,67	51,71
‹H-Me-MP (°)	12,27*	8,92*	16,71*	11,13*	13,65*	10,32*	15,09*
‹HGo-HMe (°)	144,23*	133,85*	154,07*	141,39*	147,12*	138,44*	149,92*
Patients of the main group of the 2st subgroup							
H-S (mm)	87,72*	81,18*	93,66*	85,03*	88,97*	83,30*	91,14*
H-C_{III} (mm)	26,68*	24,21*	29,52*	25,21*	27,90*	24,87*	28,93*
H-RGn (mm)	31,87*	29,27*	34,81*	31,19*	32,95*	30,56*	33,48*
H-MP (mm)	8,23*	5,38*	10,85*	7,34*	8,86*	6,53*	9,37*
H-N (mm)	126,52	108,83	135,97	121,38	130,44	115,90	134,05
H-A (mm)	80,69	67,74	88,43	75,08	83,58	72,12	85,82
H-B (mm)	45,19	28,67	53,01	40,17	48,31	34,94	50,56
‹H-Me-MP (°)	12,76*	9,41*	16,63*	11,47*	13,84*	10,59*	15,22*
‹HGo-HMe (°)	143,59*	134,06*	153,79*	141,52*	147,04*	138,61*	150,11*

Note: * – reliability of statistical differences at the level of $p \le 0.05$ by the Mann-Whitney criterion in relation to the comparison group.

As the cephalometric analysis of the head TRG (lateral projection) revealed, patients with physiological occlusion, if compared to the main group (Subgroup 1 and 2), featured the predominance of the following parameters relative to the hyoid bone body (H): the distance to the central point of the Turkish saddle (H-S) - by 14.55% and 13.69% (reliably identified, $p \le 0.05$); the distance to the lower point of the anterior edge of the third cervical vertebra body (H- CIII) - by 25.42% and 26.05% (reliably identified, $p \le 0.05$); the distance to the posterior point of the chin symphysis (H-RGn) - by 21.91% and 22.57% (reliably identified, $p \le 0.05$); the distance to the mandible body base plane (H-MR) - by 47.57% and 54.76% (reliably identified, $p \le 0.05$); the distance to the distally located point on the anterior contour of the mandible apical base (H-B) - by 6.56% and 8.26% (unreliable, $p \ge 0.05$); the angular values of the inclination to the mandible body base plane of the (‹H-Me-MP) – by 34.98% and 32.38% (reliably identified, $p \le 0.05$).

During that, children with physiological occlusion, if compared with the main group (Subgroup 1 and 2), had a decrease in such indicators as the distance from the hyoid bone body to the anterior point of the nasolabial suture (H-N) – by 6.33% and 5.25% (unreliable, $p \ge 0.05$); the distance from the hyoid bone body to the distal point on the anterior contour of the upper jaw apical base (H-A) - by 6.44% and 5.89% (unreliable, $p \ge 0.05$); the position angle of the hyoid bone body relative to the plane of the lower jaw body base (‹HGo-HMe) - by 10.34% and 9.94% (reliably identified, $p \le 0.05$).

An assessment of the hyoid bone topography in children diagnosed with distal occlusion, compared with patients featuring physiological occlusions, indicates a statistically significant ($p \le 0.05$) reduction in the distance between the mandible body and the hyoid bone body, as well as its retrograde (posterior) position relative to the plane of the mandible body base (upward and posterior displacement of the hyoid bone body) (Fig. 4-6).

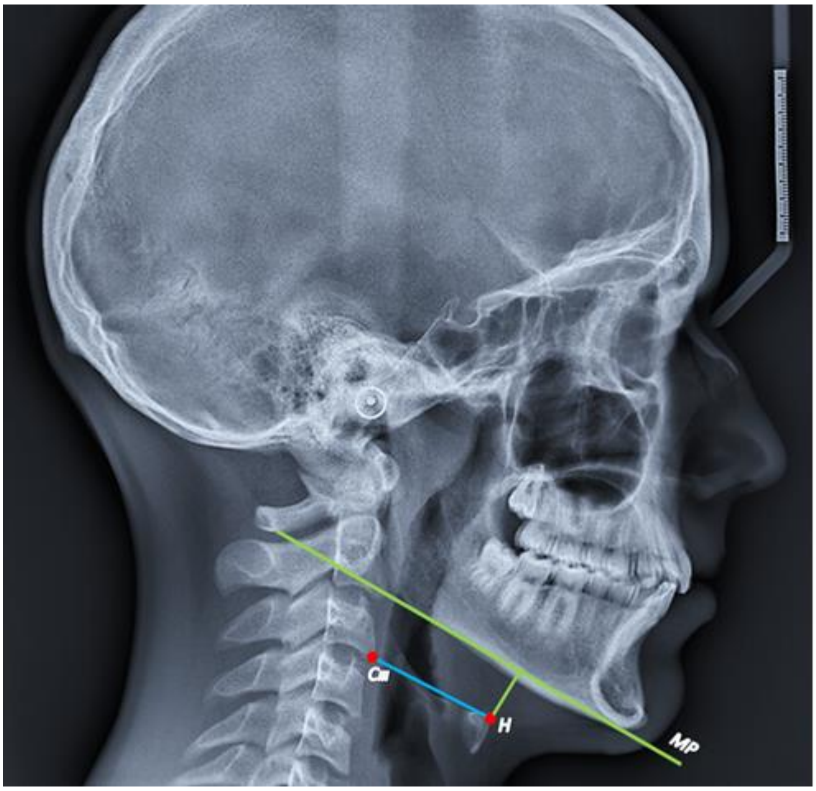

Fig. 4. Linear parameters of H-C_{III} and H-MP on TRG of the head in lateral projection of patient R., 17 years old, with physiologic occlusion.

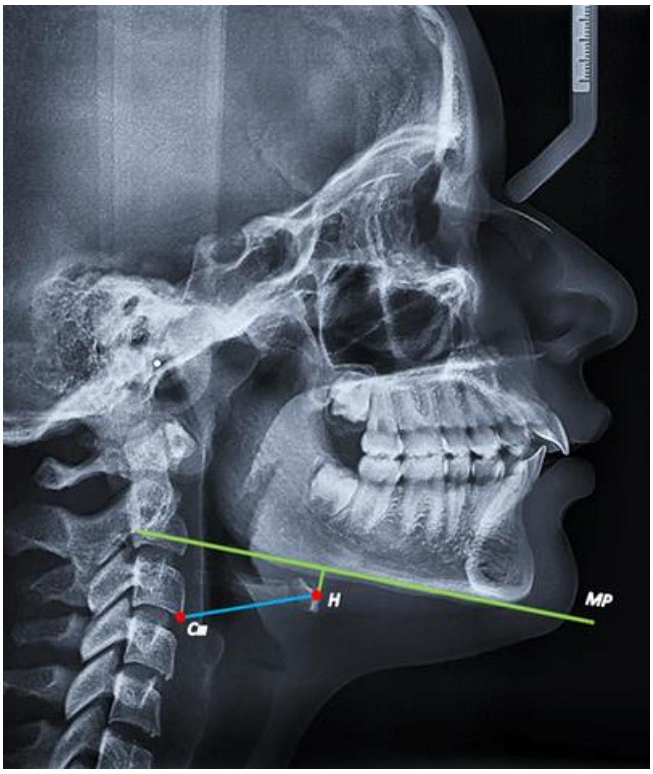

Fig. 5. Linear parameters of H-C_{III} and H-MP on TRG of the head in lateral projection of patient K., 16 years old, with distal occlusion accompanied by sagittal incisal dysocclusion.

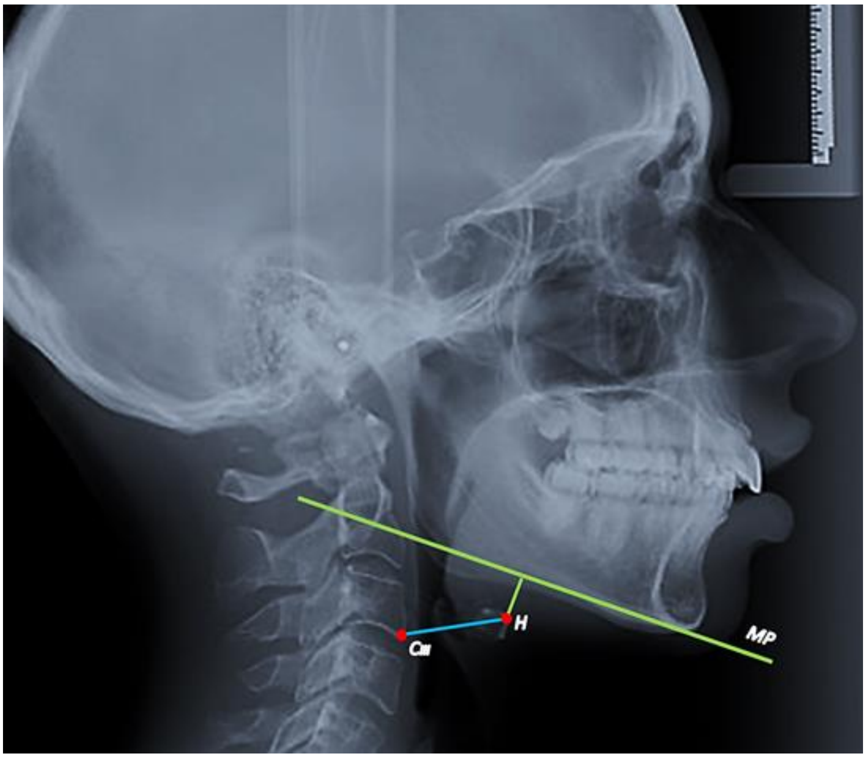

Fig. 6. Linear parameters of $H\text{-}C_{III}$ and H-MP on head TRG in lateral projection of patient A., 15 years old, with distal occlusion accompanied by deep incisal dysocclusion.

In case of the skeletal distal occlusion (‹ANB exceeding 4º), related to sagittal malocclusion due to inferior retrognathia relative to the skull anterior base or functional insufficiency of the facial and masticatory muscles, a mesial location of the upper jaw, if compared with the lower one, was diagnosed with a significant ($p \le 0.05$) increase in its length (A^{*}-SnP), as well as displacement of the mandibular body backward (distally) due to decreased parameters ($p \ge 0.05$) of the mandibular angle (Go). A statistically significant ($p \le 0.05$) shift of the hyoid bone is associated with the mandible movement, both vertically (upward) and horizontally (backward with rotation).

According to the analysis of the hyoid bone topography (H) relative to the tongue, measured by the perpendicular length from its uppermost and anterior point to the C_{III}-Me line (Rocabado M., 1984), 94.1% of children (n=32) in the comparison group were found to have the values of the perpendicular length (5.0±2.0 mm) within normative values, while patients of the main group (Subgroup 1 and 2) revealed reference intervals in 80.5% (n=33) and 80.0% (n=28) of cases, respectively.

5. Conclusions

The differentiated values of the linear, index and angular parameters of the head TRG in the lateral projection identified through cephalometric analysis in children aged 15-17 years with distal occlusion allow full assessment the nature of the disturbances affecting the facial skull morphology, as well as the intensity of skeletal pathology. This category of patients features a distal position of the lower jaw in relation to the skull anterior base (‹SNB by Me 73.05°-76.12°; $p \le 0.01$), an increase in the maxillary angle ‹ANB by Me up to 4.89°-6.95° ($p \ge 0.05$), as well as an increase in overjet by Me up to 6.61 mm ($p \leq 0.05$) in Class II of Subclass I, and an overbite by Me up to 6.75 mm ($p \leq 0.05$) in Class II of Subclass II.

Clinical and radiological explanation, approbation of the linear (H-S, H-CIII, H-RGn, H-MP, H-N, H-A, H-B) and the angular (‹H-Me-MP, ‹HGo-HMe) informative and diagnostically significant head TRG parameters, obtained while employing craniometric points, allow an objective assessment of the topography of the os hyoideum and its associated structures not in relation to the skull anterior base only (vertical), yet also to the cervical spine (horizontal).

An altered topography of the hyoid bone (H) in patients aged 15-17 years with distal occlusion, accompanied by sagittal and deep incisive disocclusion, can be observed in the vertical and horizontal directions. As could be seen from the cephalometry of the lateral head TRG, the children of the main group (Subgroup 1 and 2), if compared with the patients with physiological occlusion, had the vertical movement of os hyoideum, which was obvious from a significant ($p \leq 0.05$) decrease by Me of H-S linear values – 1.17 and 1.16 times; H-RGn – 1.28 and 1.29 times; H-MP - 1.91 and 1.83 times; the angular H-Me-MP value – 1.54 and 1.48 times; while the horizontal os hyoideum shift serves proof to a significant ($p \leq 0.05$) decrease in the H-C_{III} distance – 1.34 and 1.35 times with an increase in the HGo-NM angle – 1.16 and 1.11 times, respectively.

The detected upper and posterior displacement of the hyoid bone in patients with gnathic distal occlusion, combined with a decrease in the distance to the mandible plane (body), is one of the key pathogenetic factors behind upper respiratory tract obstruction and nocturnal apnea (Fig. 7-9).

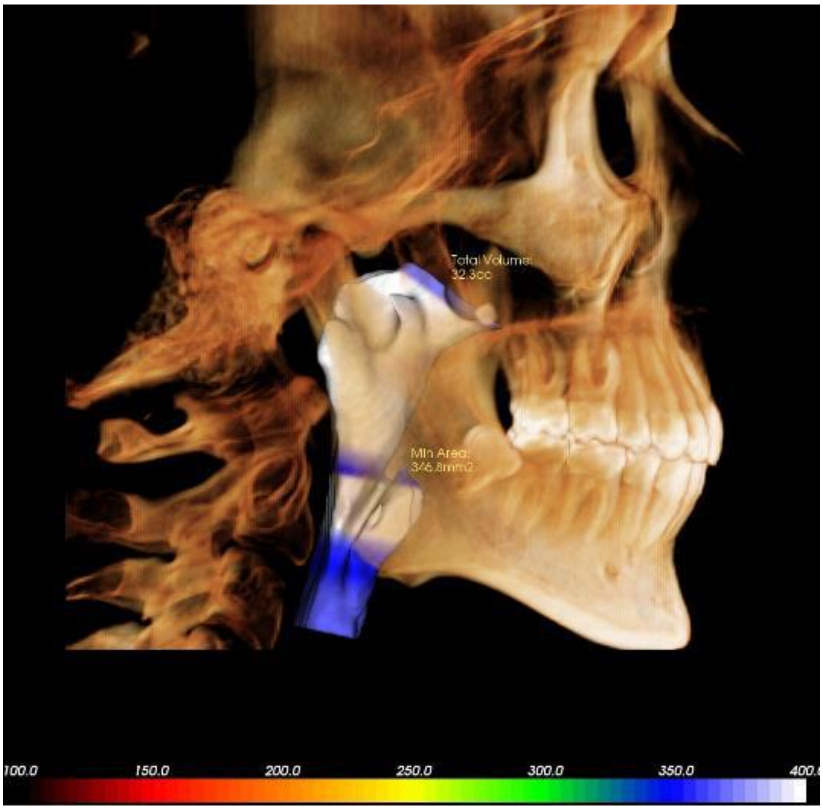

Fig. 7. 3D reconstruction of the upper airway of patient B., 17 years old, with physiologic occlusion. Airway volume is within normal limits.

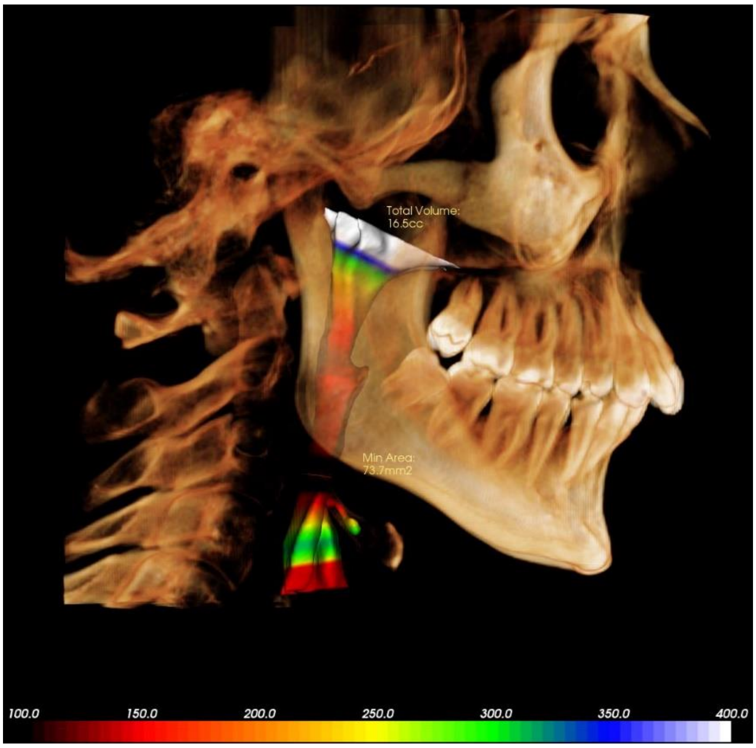

Fig. 8. 3D reconstruction of the upper airway of patient O., 17 years old, with distal occlusion accompanied by sagittal incisal dysocclusion. Airway restriction at the level of C_{I} - C_{III} vertebrae.

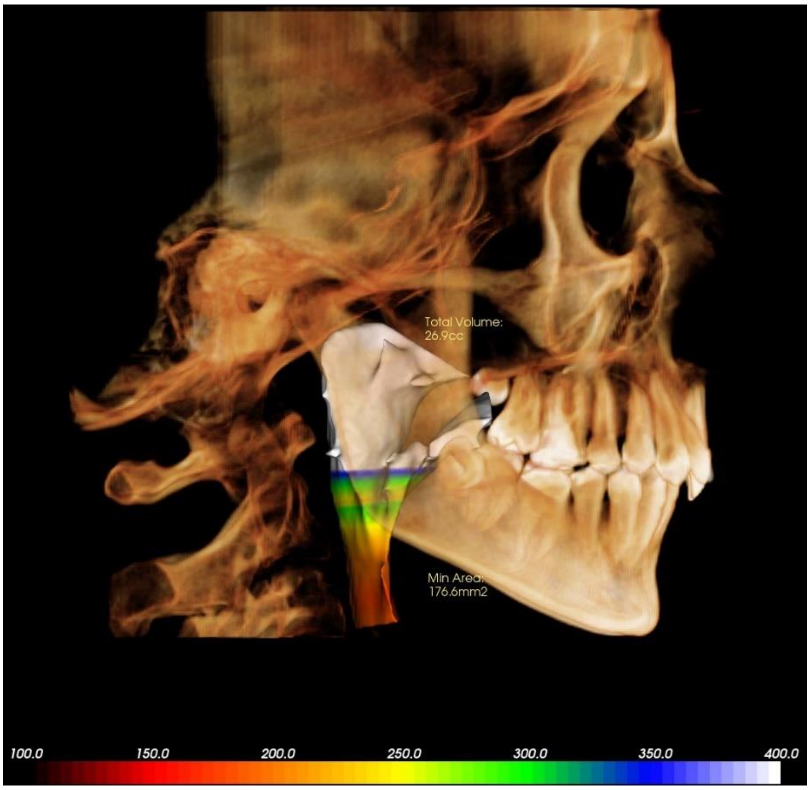

Fig. 9. 3D reconstruction of the upper airway of patient D., 16 years old, with distal occlusion accompanied by deep incisal dysocclusion. Restriction of the airway at the level of the C_{III} vertebrae.

Application of artificial intelligence:

The article is written without the use of artificial intelligence technologies.

Informed Consent Statement: Informed consent was obtained from all subjects involved in the study.

Conflicts of Interest: The authors declare no conflict of interest.

References

1. Grauer D, Cevidanes LS, Styner MA, Ackerman JL, Proffit WR. Pharyngeal airway volume and shape from cone-beam computed tomography: relationship to facial morphology. Am J Orthod Dentofacial Orthop. 2009 Dec;136(6):805-14.
2. Dmitrienko S, Domenyuk D, Tefova K. Modern x-ray diagnostics potential in studying morphological features of the temporal bone mandibular fossa. Archiv EuroMedica. 2020;10(1): 118-127.
3. Domenyuk DA, Sumkina OB, Dmitrienko S.V. Histological and morphometric studies of bone tissue autografts from intraoral and extraoral donor zones. Archiv EuroMedica. 2023;13(2):215.
4. Domenyuk DA, Sumkina OB, Mikutskaya N. Histomorphometric assessment of architectonics and vascularization in maxillary alveolar process bone tissue. Archiv EuroMedica. 2023;13(3):308.
5. Domenyuk DA, Dmitrienko SV, Domenyuk SD. Structural arrangement of the temporomandibular joint in view of the constitutional anatomy. Archiv EuroMedica. 2020;10(1): 128-138.
6. Hong JS, Oh KM, Kim BR. Three-dimensional analysis of pharyngeal airway volume in adults with anterior position of the mandible. Am J Orthod Dentofacial Orthop. 2011 Oct;140(4):e161-9.
7. Kochkonyan TS, Davydov BN. Features of the structure of the cervical spine and head position in children with anomalies of occlusion associated with connective tissue dysplasia. Part I. Institute of Dentistry. 2023;4(101):22-25.(In Russ.).
8. Di Carlo G, Polimeni A, Melsen B. The relationship between upper airways and craniofacial morphology studied in 3D. A CBCT study. Orthod Craniofac Res. 2015 Feb;18(1):1-11.
9. Ahn HN, Jeon EY, Park SB. Three-Dimensional Analysis of the Pharyngeal Airway According to Craniofacial Morphology. Iran J Public Health. 2023 Oct;52(10):2225-2227.
10. Sato K, Shirakawa T, Sakata H. Effectiveness of the analysis of craniofacial morphology and pharyngeal airway morphology in the treatment of children with obstructive sleep apnoea syndrome. Dentomaxillofac Radiol. 2012 Jul;41(5):411-6.
11. Katyal V, Pamula Y, Martin AJ. Craniofacial and upper airway morphology in pediatric sleep-disordered breathing: Systematic review and meta-analysis. Am J Orthod Dentofacial Orthop. 2013 Jan;143(1):20-30.e3.
12. Domenyuk DA, Kochkonyan TS, Shkarin VV. Conceptual approach to diagnosing and treating dentoalveolar transversal divergent occlusion. Archiv EuroMedica. 2022;12(3): 25.
13. Machado AJJr., Crespo AN. Cephalometric evaluation of the airway space and hyoid bone in children with normal and atypical deglutition: correlation study. Sao Paulo Med J. 2012;130(4):236-41.
14. Machado Júnior AJ, Crespo AN. Radiographic position of the hyoid bone in children with atypical deglutition. Eur J Orthod. 2012 Feb;34(1):83-7.
15. Domenyuk DA, Kochkonyan TS, Shkarin VV. X-ray cephalometric features of nasal and gnathic sections in different facial skeleton growth types. Archiv EuroMedica. 2022;12(4): 14.
16. Katyal V, Pamula Y, Daynes CN. Craniofacial and upper airway morphology in pediatric sleep-disordered breathing and changes in quality of life with rapid maxillary expansion. Am J Orthod Dentofacial Orthop. 2013 Dec;144(6):860-71.
17. Domenyuk DA, Kochkonyan TS, Dmitrienko SV. Periodontal tissue morphology in children with abnormal occlusion and connective tissue dysplasia syndrome. Archiv EuroMedica. 2022;12(5): 18.
18. Suetenkov DE, Firsova IV, Kubaev A. A modified method for rapid palatal expansion anchored on mini-implants. Archiv EuroMedica. 2022;12(1): 84-90.
19. Pirilä-Parkkinen K, Löppönen H, Nieminen P. Cephalometric evaluation of children with nocturnal sleep-disordered breathing. Eur J Orthod. 2010 Dec;32(6):662-71.
20. Stuck BA, Neff W, Hörmann K. Anatomic changes after hyoid suspension for obstructive sleep apnea: an MRI study. Otolaryngol Head Neck Surg. 2005 Sep;133(3):397-402.
21. Vilaza L, Araya-Diaz P, Palomino HM. Two-dimensional and Three-dimensional Assessment of the Upper Airway Int J Morphol. 2017;35(1): 357-362.
22. Solow B, Skov S, Ovesen J. Airway dimensions and head posture in obstructive sleep apnoea. Eur J Orthod. 1996; 18(6):571-579.
23. Kim SJ, Kim YS, Park JH. Cephalometric predictors of therapeutic response to multilevel surgery in patients with obstructive sleep apnea. J Oral Maxillofac Surg. 2012 Jun;70(6):1404-12.
24. Vizzotto MB, Liedke GS, Delamare EL. A comparative study of lateral cephalograms and cone-beam computed tomographic images in upper airway assessment. Eur J Orthodont. 2012;34(3): 390-393.
25. Avanisyan V, Al-Harazi G, Kondratyeva T. Morphology of facial skeleton in children with undifferentiated connective tissue dysplasia. Archiv EuroMedica. 2020;10(3):130-141.

26. Dmitrienko TD, Domenyuk DA, Porfyriadis MP. Connection between clinical and radiological torque of medial incisors at physiological occlusion. Archiv EuroMedica. 2019;9(1):29-37.

27. Shkarin VV, Grinin VM, Khalfin RA. Specific features of transversal and vertical parameters in lower molars crowns at various dental types of arches. Archiv EuroMedica. 2019;9(2): 174-181.

28. Chiang CC, Jeffres MN, Miller A. Three-dimensional airway evaluation in 387 subjects from one university orthodontic clinic using cone beam computed tomography. The Angle Orthodontist. 2012;82(6):985-992.

29. Harutyunyan Yu, Kondratyeva T, Dmitrienko SV. Undifferentiated connective tissue dysplasia as a key factor in pathogenesis of maxillofacial disorders in children and adolesce. Archiv EuroMedica. 2020;10(2): 83-94.

30. Zheng ZH, Yamaguchi T, Kurihara A. Three-dimensional evaluation of upper airway in patients with different anteroposterior skeletal patterns. Orthod Craniofac Res. 2014 Feb;17(1):38-48.